Journal of Applied Polymer Science

Oxidation and Adsorption of Arsenic Species by means of Hybrid Polymer Containing Manganese Oxides

Daniel Ociński, Irena Jacukowicz-Sobala, Elżbieta Kociołek-Balawejder
Department of Industrial Chemistry, Wroclaw University of Economics, 53-345 Wrocław, Poland
Correspondence to: D. Ociński (E-mail: daniel.ocinski@ue.wroc.pl)

ABSTRACT: The aim of this work was a comprehensive study of the oxidative and sorptive properties of a hybrid polymer containing manganese oxide toward As(III) and As(V). A poly(styrene-divinylbenzene) copolymer containing oxidative functional groups (—SO_2NBrNa) was used as the supporting material for MnO_2. The inorganic component was deposited as a result of the oxidation reaction of Mn(II) with oxidative groups of the host polymer. The surface of the polymer matrix was evenly covered with a thin layer of manganese oxide. The obtained product (R/S/Mn) exhibited high oxidative capacity over a wide pH range (2–12); however, under acidic and neutral conditions, the reaction ran significantly faster. The studied material shows some sorption properties but its sorption capacity is much lower than its oxidation capacity. The treatment, in a column regime, of the arsenic solution containing 1 mg As(III) dm^{-3} and coexisting ions in concentrations similar to those in natural waters, confirmed the excellent oxidation capacity of the obtained product. © 2013 Wiley Periodicals, Inc. J. Appl. Polym. Sci. **2014**, *131*, 39489.

KEYWORDS: oxidation; adsorption; applications; composites; functionalization of polymers

Received 26 February 2013; accepted 1 May 2013
DOI: 10.1002/app.39489

INTRODUCTION

Arsenic is a naturally occurring element in the environment well known for its toxicity and carcinogenicity that enters the natural aqueous systems by leaching from minerals and soils. Long-term exposure to As compounds in drinking water causes a variety of diseases, including cancer of the liver, lung, kidney, bladder and skin as well as pigmentation changes, skin thickening, and neurological disorders. In accordance with the WHO recommendation, during the last decade in many countries, the maximum contaminant level of arsenic in drinking water was lowered from 0.05 to 0.01 mg dm^{-3}. In many regions of the world, the concentration of arsenic in drinking water sources exceeds the acceptable level, causing serious health problems.[1–4] Arsenic exists in natural waters mainly in the form of inorganic species—arsenates (As(V)) and arsenites (As(III)), which differ markedly in terms of toxicity and mobility. As(III) is more toxic than As(V) due to its high affinity for sulfhydryl groups in proteins. In water, below pH 9, arsenites appear mainly in the form of undissociated molecules (H_3AsO_3), while arsenates exist under these conditions as a mixture of oxyanions ($HAsO_4^{2-}$, $H_2AsO_4^-$). In consequence, dissociated As(V) compounds are less mobile in the natural environment due to electrostatic interactions with environmental constituents such as minerals, soils, and sediments than undissociated and more toxic As(III) compounds. This is also the cause of lower efficiency of As(III) removal from waters by most existing technologies (coagulation, adsorption, and ion exchange). Therefore, oxidation of As(III) to As(V) is required as a pretreatment step for efficient removal of total arsenic from waters. It can be achieved by using homogeneous oxidants, that is, chlorine, hypochlorite, hydrogen peroxide, ozone, permanganate, or peroxydisulfate, but they may cause some problems arising from the presence of residual oxidants or from formation of byproducts.[5–10] Oxidation of As(III) by dissolved oxygen does not cause any environment threats but is kinetically slow.[10,11] An alternative way of As(III) to As(V) conversion is photochemical oxidation in the presence of TiO_2 and dissolved iron/sulfite species as photocatalysts or other advanced oxidation processes combining hydrogen peroxide or ozone with ultraviolet radiation.[10,12–16] Furthermore, some studies concern the techniques combining the electrochemical oxidation of As(III) with the removal of As(V) mainly by coagulation and membrane processes.[17–19] As the most suitable technique for treatment of diluted solutions is adsorption, a significant number of studies focused on the use of heterogeneous oxidants converting As(III) to As(V) before the removal process. A special effort has been made to develop materials containing manganese oxides, both natural and synthetic, or Fe-Mn binary oxides.'[9,10,12,20–22] They exhibit excellent oxidative properties toward As(III) and, under certain conditions, show some adsorption capacity to As(III) and As(V). A significant

drawback of such materials is their physical form resulting in high hydraulic resistance of the bed in column processes. To overcome this inconvenience, one can coat some solid materials with good hydraulic properties, for example, sand, with manganese oxides.[23] While the obtained materials can be used in the form of a fixed bed in column processes, their surface area and oxidation capacity is significantly lower than manganese oxide particles. Better results may be achieved by incorporating manganese oxides into macroporous, organic reactive polymers with ionic functional groups (ion exchangers). The advantages of these materials are excellent hydraulic and mechanical properties, insolubility in water, and a high surface area. Due to the presence of reactive, functional groups in the polymer matrix, the inorganic deposit (manganese oxides) may be easily introduced and evenly dispersed within the polymeric material. The product—hybrid polymer—combines the mechanical and hydraulic properties of the host polymer with the specific sorptive/oxidative properties of an inorganic deposit. The majority of studies described in the literature concern the synthesis of hybrid polymers with dispersed iron oxides, used for removal of different organic and inorganic pollutants from waters.[24–28] There are only a few studies in the literature that investigate the possibility of synthesis and use of polymers containing manganese oxide as a sorbent and heterogeneous oxidant for toxic water contaminants such as arsenic, cadmium, lead, or radionuclides.[29–33]

In this study as the host material for manganese oxide deposition, we used S/DVB (poly(styrene-divinylbenzene)) polymer having $-SO_2NBrNa$ oxidizing functional groups. In previous research works, this macromolecular oxidant was tested in water treatment processes to remove many aqueous contaminants, for example, manganese(II).[34] It was shown that carrying out the water demanganization process under controlled pH conditions led to manganese(IV) oxide precipitation within matrix of the polymeric reagent.[35] The aim of this study was to evaluate the oxidation of As(III) as a pretreatment step in arsenic removal processes using hybrid polymer containing manganese oxide as the heterogeneous oxidant. The advantage of this material is a combination of the porous structure of the polymeric constituent and high oxidizing capacity of the inorganic deposit, which enables this process to be carried out in fixed-bed column systems. Since, according to literature data, manganese oxide is a good adsorbent, we also tested sorption properties of the obtained hybrid polymer toward As(III) and As(V) compounds.

EXPERIMENTAL

Reagents

All reagents used were of analytical grade. Solutions were prepared with deionized water (18.3 MΩ cm^{-1}; Barnstead, EASYpure RF). The arsenite and arsenate stock solutions (1000 mg As dm^{-3}) were prepared from sodium (meta)arsenite $NaAsO_2$ (Sigma-Aldrich, ≥99% purity) and disodium hydrogen arsenate $Na_2HAsO_4 \times 7H_2O$ (Sigma-Aldrich, ≥98% purity), respectively. A solution of $MnSO_4 \times H_2O$ (Chempur, Poland) was used as the reducing agent for the hybrid polymer synthesis. For pH adjusting, 0.1*M* HCl and 0.1*M* NaOH solutions were used.

Polymer resin with *N*-bromosulfonamide functional groups was prepared in accordance with the method described previously:[36]

$$[P]-SO_3H \rightarrow [P]-SO_2Cl \rightarrow [P]-SO_2NH_2 \rightarrow [P]-SO_2NClNa \rightarrow [P]-SO_2NBrNa \quad (1)$$

As a starting material for synthesis of the redox polymer, we used the sulfonic cation exchanger Amberlyst 15 produced by Rohm and Haas, which is a macroporous S/DVB resin containing 4.7 mmol $-SO_3H$ g^{-1}; surface area 45 m^2 g^{-1}; average pore diameter 25 nm; uniformity coefficient <1.70; harmonic mean size 600–850 μm. The product of subsequent reactions in the air dried state contained 1.65 mmol g^{-1} $-SO_2NBrNa$ groups (the decrease of the functional groups content was mainly a result of the increase of polymer density due to larger molar mass of $-SO_2NBrNa$ groups in comparison to $-SO_3H$ groups) and 0.5 mmol g^{-1} of residual $-SO_3Na$ groups.

Preparation and Characterization of the Hybrid Polymer

Synthesis. The synthesis was carried out in a batch regime: a 10 g dried sample of the resin was placed in a flask and treated with 0.07*M* $MnSO_4$ solution (700 cm^3). The flask was closed airtight and shaken at 22°C in the dark for 24 h. The resulting suspension was then filtered and the resin was thoroughly washed with water and 200 cm^3 of methanol. The obtained product (R/S/Mn) was dried at 60°C for 24 h. A portion of resin was additionally neutralized by washing with 1*M* NaOH.

Characterization of the Hybrid Polymer. To determine the Mn content in the polymer matrix, 0.1 g of hybrid polymer sample was treated for 24 h with 15 cm^3 of 7.5*M* HNO_3. The obtained solution was analyzed using inductively coupled plasma atomic emission spectroscopy (ICP-AES) (Varian Liberty). Microscopic examinations were performed by means of a HITACHI S-3400N scanning electron microscope (SEM) equipped with an energy dispersive X-ray spectroscopy (EDS) microanalyzer (4 nm, BSE detector). Specific Brunauer-Emmett-Teller (BET) surface area and the porous characteristics of the hybrid polymers were determined from the adsorption isotherms for liquid nitrogen at 77K using Accelerated Surface Area and Porosimetry Analyzer ASAP 2020, 2007, Micrometrics.

The pH_{zpc} (point of zero charge) of the hybrid polymer was determined by means of the drift method.[37] Measured amounts of the product (0.1 g) were contacted for 24 h with 1*M* KCl solutions of initial pH in the range 2–11. After that time, the final pH of the solutions was measured and the graph of the initial pH versus ΔpH was plotted. The point at which the curve crossed the pH-axis determined the pH_{zpc} of the polymer.

Measurements

Arsenic concentration was determined using the spectrophotometric molybdenum blue method (Specord 210, Analytical Jena, Germany) with the absorbance measurement at 880 nm.[38] Because arsenite does not form the molybdenum complex, to determine the total arsenic concentration, prior to the analysis an oxidizing agent (potassium iodate) was used to convert As(III) into As(V). The arsenite concentration was calculated as

the difference between the total arsenic concentration and the arsenate concentration.[39] In the case of arsenic concentration lower than 0.05 mg dm^{-3} hydride generation atomic absorption spectrometry with a graphite tube (AAS Avanta) or ICP-AES (Varian Liberty) was used. Because these methods enable one to determine only the total arsenic concentration, As(III) and As(V) were first separated using the strong base anion exchanger (Amberlite IRA 402Cl), after adjusting the pH to 4.0.[40]

Determination of manganese concentration in solutions was carried out using ICP-AES (Varian Liberty).

Oxidation Studies

Oxidation experiments were performed in both batch and column regimes, using an IKA KS-260 control shaker and the Gilson MiniPuls3 peristaltic pump with the FC204 Fraction Collector, respectively.

The effect of pH on arsenite oxidation was conducted by shaking 0.5 g of the hybrid polymer with 50 cm^3 of 0.00125*M* $NaAsO_2$ (93 mg As(III) dm^{-3}) in 0.01*M* H_2SO_4, 0.01*M* NaOH and in water for 24 h. The oxidation kinetics were carried out for various arsenite concentrations (25, 100, 220 mg As(III) dm^{-3}) and various heterogeneous oxidant doses (0.1, 0.25, 0.5 g). The arsenite solutions were shaken in Erlenmeyer flasks with the sample of hybrid polymer for 24 h, and the concentration of arsenate was analyzed in appropriate time intervals. The effect of various competing ions, such as sulfates, phosphates, chlorides, bicarbonates, and calcium, was assessed using 10 m*M* solutions of particular ions (for phosphates additionally 0.1 m*M*) containing 5 mg As(III) dm^{-3} at pH established at about 7.5. A sample of hybrid polymer (0.1 g) was shaken for 24 h in an Erlenmeyer flask with 40 cm^3 of appropriate solutions.

The column study was conducted by passing the arsenite solution with concentration of 1.0 mg As(III) dm^{-3} containing some competing ions (60 mg SO_4^{2-} dm^{-3}, 0.31 mg PO_4^{3-} dm^{-3}, 100 mg HCO_3^- dm^{-3}, 164.5 mg Cl^- dm^{-3}, 60 mg Ca^{2+} dm^{-3}, 20 mg Mg^{2+} dm^{-3}) through the hybrid polymer bed (5 g) at a flow rate of 6 bed volumes h^{-1}. The collected fractions of the effluent were analyzed in terms of pH, arsenite and total manganese concentrations.

Adsorption Studies

Adsorption experiments were performed in a batch regime using an IKA 260 control shaker. The effect of pH on the sorption of As(III) and As(V) by means of the obtained hybrid polymer was analyzed similar to oxidation studies, but with the use of 0.01*M* and 0.001*M* H_2SO_4, 0.001*M* NaOH and water alone as the reaction medium. The adsorption kinetics studies were carried out by shaking 1.0 g of the sorbent with 100 cm^3 of different arsenite and arsenate concentrations of either 10 and 100 mg dm^{-3}. Isotherm studies were performed by shaking 40 cm^3 of solution containing different arsenic concentration between 1 and 100 mg As(III) dm^{-3} and between 1 and 50 mg As(V) dm^{-3} with 0.25 g of the hybrid polymer at neutral pH. The effect of various competing ions on As(III) adsorption effectiveness was studied similarly to oxidation experiments.

RESULTS AND DISCUSSION

Synthesis and Characterization of Adsorbent

Reactions of Mn(II) oxidation using redox S/DVB polymers containing various *N*-halogenosulfonamide functional groups were described in previous studies.[34,41] These experiments showed that *N*-bromosulfonamide polymer exhibited high oxidation capacity toward Mn(II) and the product of this reaction was deposited with the highest yield in the form of manganese oxide within the polymer matrix in comparison with other studied redox polymers:

$$[P]-SO_2NBrNa+MnSO_4+2\,H_2O \rightarrow [P]-SO_2NH_2+MnO_2(\downarrow)+NaBr+H_2SO_4 \quad (2)$$

To obtain a homogeneous product, incorporation of the inorganic deposit was carried out under batch conditions. As a result, we obtained a hybrid polymer with the appearance of gray beads and containing 7.3% (w/w) of manganese. Table I presents characteristics of the hybrid polymer and the host polymer containing sulfonamide functional groups which were also present in the hybrid material as a result of the oxidation–reduction reaction with Mn(II). Both materials also contained small numbers of residual sulfonic groups which were formed in a side reaction during conversion of $-SO_2Cl$ groups into $-SO_2NH_2$ groups (1). The sulfonamide groups with $pK_a > 11.0$, in contrast to cationic or anionic functional groups of ion exchange hybrid polymers presented in the literature, are not dissociated over a wide pH range.

Table I. Characteristics of Polymeric Materials—Supporting Material and Product

	Sulfonamide copolymer	Sulfonamide copolymer containing manganese oxide
Sample code	R/S	R/S/Mn
Polymer matrix	S/DVB[a]	S/DVB[a]
Chemical constitution	$-SO_2NH_2$	$-SO_2NH_2$#MnO_2[b]
Main functional group (mmol g^{-1})	3.9	1.85[c]
Residual $-SO_3^-$ group (mmol g^{-1})	0.5	0.23[c]
Mn content (%)	-	7.3
BET surface area (m^2 g^{-1})	48.02	49.0
Total pore volume (cm^3 g^{-1})	0.15	0.17
Average pore diameter (nm)	12.54	14.21

[a] Macroporous styrene-divinylbenzene copolymer.
[b] # - MnO_2 deposited within polymer matrix.
[c] Assessment based on mass comparison before and after reaction of Mn(II) oxidation (constant mass).

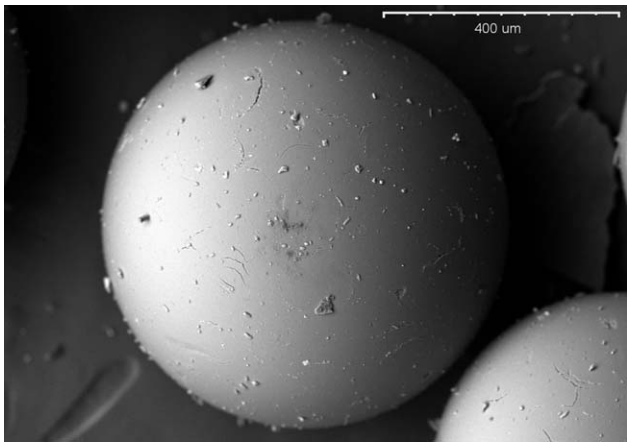

Figure 1. SEM image of the bead of the R/S/Mn polymer.

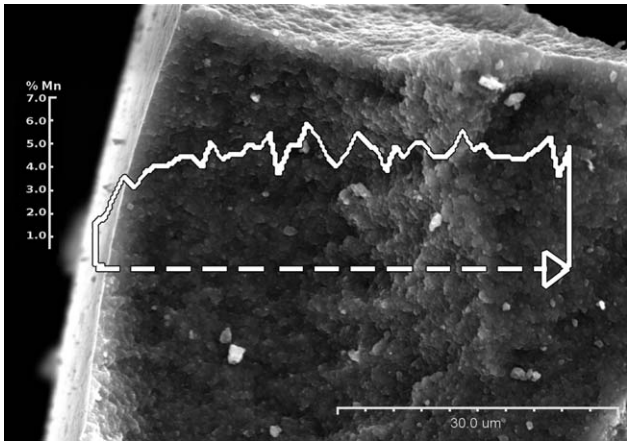

Figure 2. SEM with linear EDS analysis of the R/S/Mn polymer. The curve illustrates the changes of manganese content in the oxidant's bead section.

The aim of following instrumental analyses of the obtained product was to determine the distribution of manganese oxide within the polymer matrix, which may significantly influence its performance, such as hydraulic properties or oxidation and sorption capacity. SEM analyses presented in Figures 1 and 2 show the morphology of the hybrid polymer; in particular, in Figure 1 a single spherical bead is shown and in Figure 2 the internal structure of the fractured bead is shown. It can be observed that no manganese oxide in the form of microscale aggregates or crystals was deposited.

The presence of Mn was confirmed by the EDS analysis, which was performed both linearly and in points. These results revealed that the manganese deposit is lower on the outer surface of the beads (1.17–1.73%) than on their inner surface (3.30–5.99%) (Figure 2).

However, the Mn content at different points of the hybrid polymer is the same order of magnitude, which suggests that manganese oxide was evenly distributed in the polymer matrix. The higher manganese deposit on their inner surface is probably the result of even distribution of both *N*-bromosulfonamide and residual sulfonic functional groups within the beads of the redox polymer. Sulfonic groups due to electrostatic attraction enhance

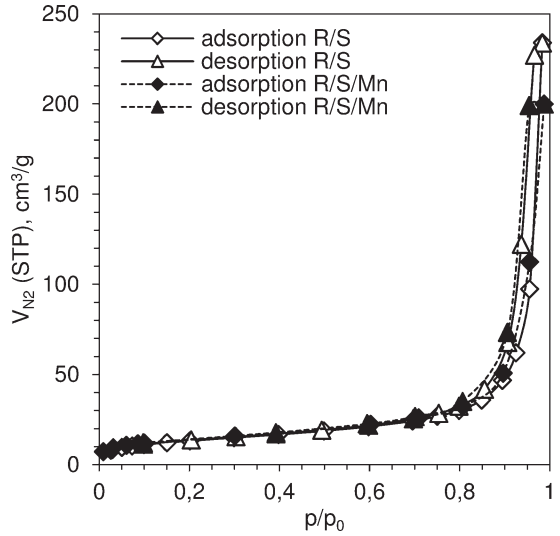

Figure 3. Isotherms of nitrogen adsorption and desorption for the R/S/Mn polymer and for the hosting sulfonamide polymer.

the transport of Mn^{2+} ions into the inner surface of the beads where the subsequent oxidation and precipitation of manganese oxide occurs.

Figure 3 shows isotherms of nitrogen adsorption/desorption on the obtained hybrid polymer and on the supporting polymer without manganese oxide deposit; their porosity characteristics are listed in Table I.

Both materials as S/DVB reactive polymers exhibited relatively high BET surface area. The analysis of the isotherms and hysteresis loops starting at p/p_0 closer to unity, which reflect the shape of type H1, indicates mesoporous structure of these materials with a narrow size distribution of cylindrical-like pores. Comparison of the S_{BET}, pore volumes and average pore diameters of the product and the host material revealed that manganese oxide deposition did not cause any changes in textural structure of the supporting polymer. These results indicated that the surface of the polymer matrix was covered with a thin film of manganese oxide.

The pH of zero charge point of the sorbent is an important parameter which influences its sorption capacity. At a pH value lower than $pH_{ZPC,}$ the sorbent surface is positively charged and under these conditions, the anion adsorption is favorable due to electrostatic attraction. The optimal pH of the sorbent performance is between its pH_{ZPC} and pK_a of the acid. As the pK_{a1} of H_3AsO_4 and H_3AsO_3 are 2.2, 9.2, respectively, a higher pH_{ZPC} value may result in higher sorption capacity toward arsenate and arsenite and a wider pH operating range of the sorbent. According to the literature data, manganese oxides of various origin exhibited pH_{ZPC} values of 3.9–4.3.[30] The point of zero charge of the obtained hybrid polymer reached a higher value of 5.8. The influence of the polymer matrix on this parameter agrees with the study on manganese oxide deposited in the matrix of anion exchanger, which exhibited an even higher value of 7.8.[30]

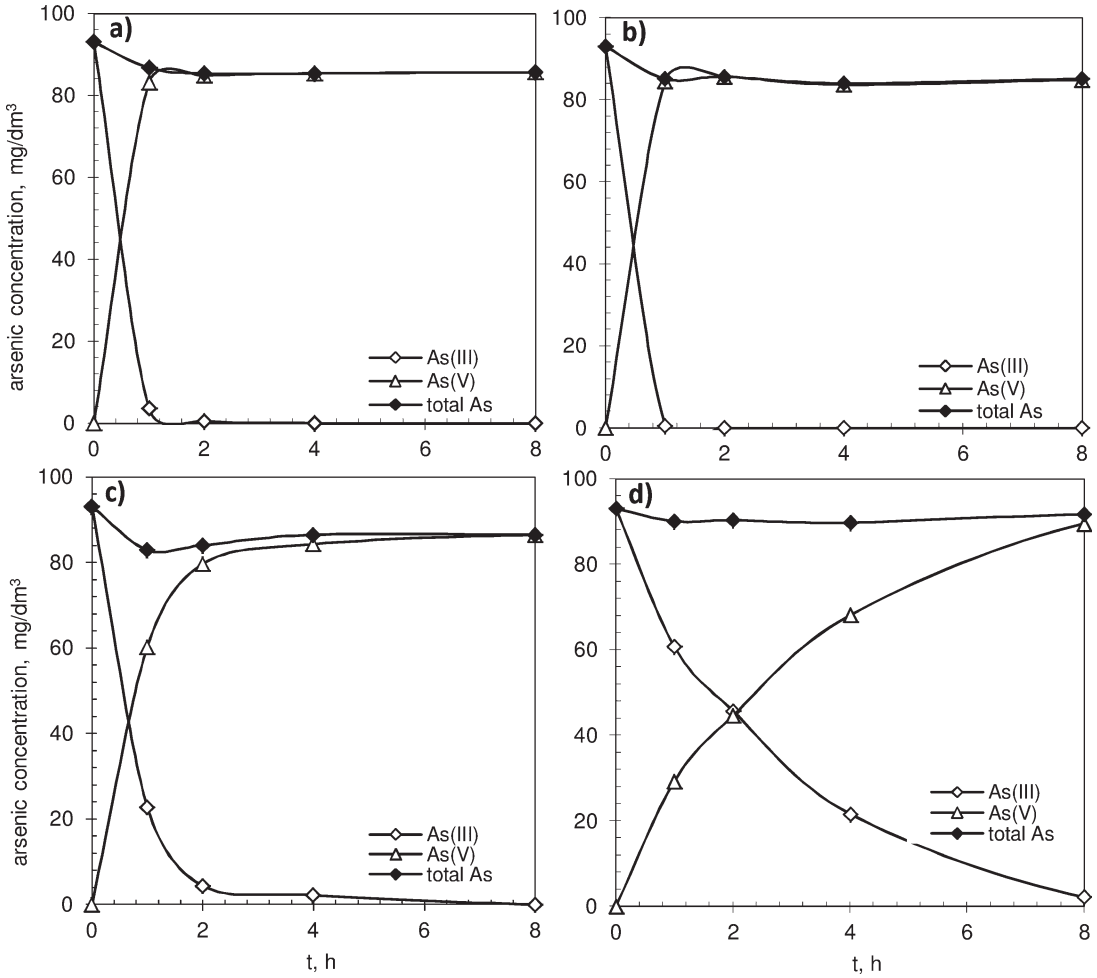

Figure 4. Kinetics of As(III) oxidation and adsorption by means of R/S/Mn polymer at various pH; a) water alone, pH = 2.76, b) 0.01 M H_2SO_4, pH = 1.95, c) water alone, pH = 6.14, and d) 0.01 M NaOH, pH = 12.01); (50 cm^3 of $NaAsO_2$ solution, 93 mg As(III) dm^{-3}, 0.5 g of the R/S/Mn).

Preliminary Batch Studies on the Oxidation and Adsorption of As(III) Under Various pH Conditions

The kinetics of As(III) oxidation and its removal under various pH conditions (final pH: 1.95, 2.76, 6.14, and 12.01) are shown in Figure 4(a–d).

The presented curves show that the obtained hybrid polymer exhibited excellent oxidative properties over a wide pH range and minor adsorptive properties in acidic and neutral environments. The oxidation reaction was very fast, particularly at the initial stage of the process. Under acidic conditions (pH 1.95 and 2.76), the total amount of arsenic in solution was converted to As(V) within the first 60 min of the reaction. At neutral pH (6.14), only 25% and 7% of nonoxidized arsenic remained in the solution after 60 and 120 min, respectively, and complete arsenic oxidation was achieved after 7 h of contact. The slowest run of As(III) oxidation reaction, also at the initial stage, was observed in the alkaline environment (pH 12.01). Despite the strongly alkaline environment unfavorable for As(III) oxidation and high arsenite concentration—exceeding by several orders of magnitude those occurring in natural waters—almost all As(III) in solution was converted to As(V) within 8 h.

The drop of pH in water alone [Figure 4(a)] may be a consequence of the manganese oxide deposition during the hybrid polymer synthesis which occurred according to reaction (2) under acidic conditions since one of its products is H_2SO_4, resulting in conversion of the residual $-SO_3Na$ groups into hydrogen form. The presence of other cations in the treated solution caused an ion exchange reaction and the release of protons from sulfonic groups. For that reason, we also used the hybrid polymer after the neutralization process [Figure 4(c,d)], whose purpose was to convert sulfonic groups into sodium form, which prevented acidification of the treated solution.

In contrast to the oxidation reaction, the effectiveness of the adsorption of As(III) on the hybrid polymer was low over the whole pH range studied. Under acidic and neutral conditions, the concentration of total arsenic in solution decreased by almost 20% after 24 h, while in an alkaline environment, the drop was practically negligible. Therefore, further studies were conducted on oxidation of arsenite (batch and column tests) and adsorption of arsenite and arsenate (batch tests), separately.

The Theory of As(III) Oxidation on the Surface of Manganese Oxides

To facilitate the interpretation and understanding of the results of our studies, the theoretical mechanism of arsenite oxidation on the solid manganese oxide surface, based on the literature review, is briefly discussed below.

The preliminary stage of As(III) to As(V) conversion is the binding of As(III) on the surface of solid manganese(IV) oxide through a complexation mechanism.[42] Then, the As(III) molecules undergo oxidation to As(V) in a two-stage process, which can be depicted in the form of the simplified, summary chemical equation:[43–47]

$$\equiv Mn^{IV}-OH+H_3AsO_3 \rightarrow Mn^{2+}+H_2AsO_4^- +2H^+ \qquad (3)$$

The formed arsenate ions are adsorbed on the surface of the oxidant, which reduces the amount of available active sites, and in consequence slows down the reaction rate.[42,48,49] This process is facilitated by the released Mn(II) ions, which can also be adsorbed on the surface of the heterogeneous oxidant, giving it a positive charge.[50,51] Simultaneously under some conditions, the precipitation of manganese arsenate may occur, resulting in reduction of the availability of the active sites on the oxidant surface.[30,45,48] Besides passivation of the surface of MnO_2 through improving As(V) sorption or manganese(II) arsenate precipitation, Mn(II) can react with superficial Mn(IV) atoms in a comproportionation reaction, which results in increase of the less reactive $Mn^{(III)}$ on the surface.[44,52] The oxidation of As(III) at the surface of manganese oxides is thus a complex process, the efficiency of which depends on various factors, both chemical and diffusive.

Oxidation Studies

The results of the studies on the oxidation of As(III) by R/S/Mn at different arsenic initial concentrations are presented as arsenite oxidation capacity in Figure 5.

The increase of the initial As(III) concentration in solution resulted in the higher oxidation capacity of the heterogeneous oxidant (mg As(III) g^{-1}), which was the consequence of excess of the arsenite toward the hybrid polymer sample, driving the reaction in the direction of products. As shown in Figure 5, the oxidation capacity of the hybrid polymer has been established at a constant level only for the lowest As(III) concentration, while for both solutions with higher initial arsenic content the oxidation capacity gradually increased in a contact time of 24 h. The highest rate of As(III) oxidation was observed at the initial stage of the reaction, followed by its distinct decrease and a plateau at the final stage. The oxidation of As(III), therefore, does not follow a pseudo-first-order kinetic well.[49] Considerably lower reaction rates in solutions with high As(III) concentrations (100, 220 mg As(III) dm^{-3}) may be the result of passivation of the active sites on the surface of MnO_2 by Mn^{2+} or As(V), formed in the oxidation reaction.

The kinetics of As(III) oxidation at various heterogeneous oxidant doses (0.1, 0.25, and 0.5 g) are shown in Figure 6.

The increase of the hybrid polymer dose obviously caused distinct enlargement of the reaction rate, due to a larger excess of the oxidizing agent. Simultaneously, the oxidation capacity of the hybrid polymer (expressed in mg As(III) g^{-1}) diminished with the increase of the oxidant dose. The reason was the smaller amount of As(III) in the solution per unit mass of the polymer. Despite the similar final efficiency of the reaction for all oxidant doses, their courses differed greatly. The slowest course of the reaction was observed for the smallest hybrid polymer dose, which may be due to the passivation of the oxidant surface, described earlier. This process naturally occurs regardless of the solid oxidant dose used, but in this case (0.1 g R/S/Mn) there is only a slight excess of the oxidant toward As(III), so any decrease of the availability of the active sites influences the reaction course, slowing it down significantly.

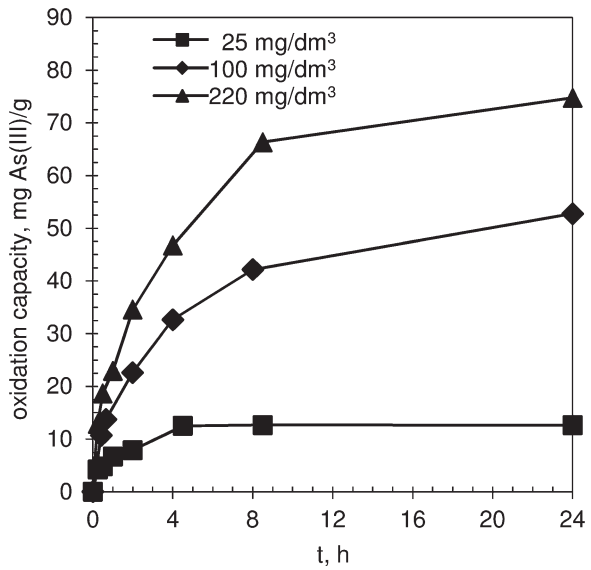

Figure 5. Effect of the initial concentration of As(III) on the kinetic of the As(III) oxidation process by R/S/Mn; (0.1 g of the R/S/Mn, 100 cm^3 of $NaAsO_2$ solutions).

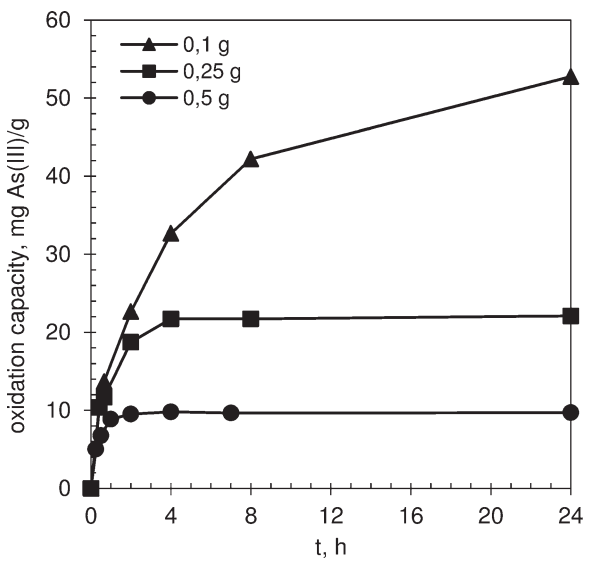

Figure 6. Effect of the heterogeneous oxidant dose on the kinetic of the As(III) oxidation process by R/S/Mn; 100 cm^3 of $NaAsO_2$ solutions (100 mg As(III) dm^{-3}).

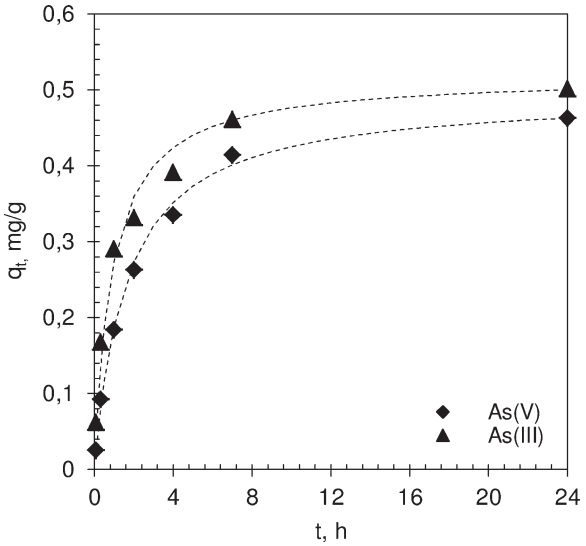

Figure 7. The kinetics of As(III) and As(V) sorption on the R/S/Mn polymer; the dashed lines are the plots of the pseudo-second-order kinetic model; 100 cm^3 of $NaAsO_2$ solutions (10 mg As(III) dm^{-3}, 1.0 g of the R/S/Mn).

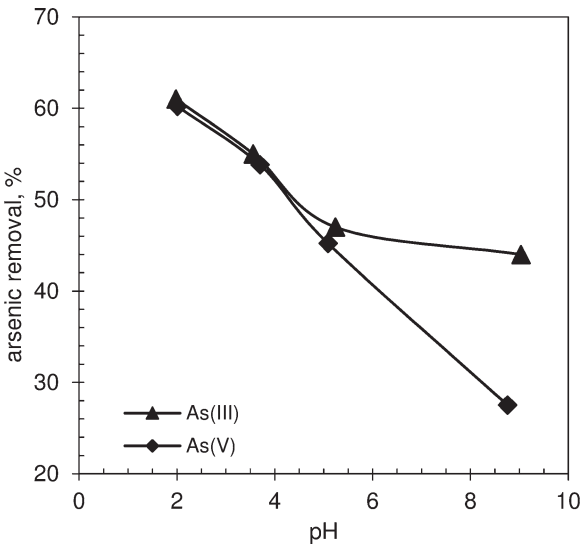

Figure 8. Effect of pH on As(III) and As(V) removal by R/S/Mn, 50 cm^3 of $NaAsO_2$ solutions (10 mg As(III) dm^{-3}, 0.5 g of the R/S/Mn).

The results confirmed that the important factor ensuring a high oxidation rate of the As(III) by means of solid manganese(IV) oxide is a proper excess of heterogeneous oxidant.[53]

Adsorption Studies

The removal and oxidation of arsenic species from aqueous solutions is a complex process which occurs by means of a multistep mechanism involving mass transfer across the external boundary layer, diffusion within the porous structure of the oxidant, sorption of the reagent molecule As(III) at the surface active sites, oxidation reaction and desorption of the product As(V). Each of these steps may be the rate controlling stage. As manganese oxide exhibits sorption capacity toward both arsenate and arsenite, the As(V) ions may permanently occupy the surface of the oxidant. To describe the mechanism of performance of the obtained hybrid polymer, we also examined its sorption capacity toward As(III) and As(V) ions separately using reaction-based and diffusion-based kinetic models and isotherm models.

As can be seen from Figure 4(a–d), sorption capacity of the hybrid polymer is significantly lower than its oxidation capacity; for this reason, the kinetic adsorption studies were carried out with high sorbent dosage of 10 g dm^{-3} and low arsenic concentration of 10 mg dm^{-3} under acidic conditions (pH = 3.5). The results (Figure 7) showed that As(III) and As(V) were removed with a comparable efficiency, reaching maximum values after 24 h of contact—50% and 46% respectively.

In the initial phase of the process (7 h), the adsorption of both adsorbates increased sharply, resulting in more than 46% As(III) and 40% As(V) removal and achieving the plateau in the second stage. As the adsorption of ions is influenced by the pH value, variation of the As(III) and As(V) sorption with pH was also studied (Figure 8). The results showed that arsenates removal was strongly dependent on pH conditions.

The acidic environment enhanced their removal due to electrostatic attraction between those anions and positively charged surface of the manganese oxide. At pH 5.0 and 9.0 which are, respectively, close to and higher than pH_{ZPC} of the hybrid polymer, the sorption capacity significantly decreased. The lower adsorption capacity under basic conditions can be explained by the competitive adsorption of hydroxide anions and the repulsion between arsenate and the negatively charged surface. The removal efficiency of As(III) species was slightly pH dependent, which could be a result of different mechanisms of their adsorption. At the studied pH range, the poorly dissociated As(III) was adsorbed in two steps: its oxidation and formation of specific inner-sphere complexes with manganese oxide. This supposition confirms the fact that As(III) removed from the bulk solution was adsorbed in the form of As(V) ions. Presumably the oxidation step was followed by arsenate desorption, manganese cations release, and subsequent arsenate adsorption. Under acidic conditions, As(V) was adsorbed on protonated active sites of manganese oxide, while at higher pH values, the negative charge of the surface was partially neutralized by Mn^{2+} sorption, which enhanced its affinity to arsenates.

The kinetic data were analyzed using pseudo-first-order and pseudo-second-order kinetic models, which are expressed as follows:[54–57]

$$dq_t/dt = k_1(q_e - q_t) \quad (4)$$

$$dq_t/dt = k_2(q_e - q_t)^2 \quad (5)$$

The integrated forms of eqs. ((7)) and ((8)) are written as:

$$\ln(q_e - q_t) = \ln q_e - k_1 t \quad (6)$$

$$t/q_t = 1/k_2 q_e^2 + t/q_e \quad (7)$$

from the eq. ((10)), the initial sorption rate may be calculated:

$$h = k_2 q_e^2 \quad (8)$$

where k_1, k_2 are the equilibrium rate constants of the pseudo-first- and pseudo-second-order adsorption models, respectively, q_e is the amount of adsorbate adsorbed at equilibrium, and q_t is the amount adsorbed at time t.

Table II. Kinetic Parameters for Arsenic Adsorption by means of R/S/Mn Polymer

	Value	
Parameter	As(III)	As(V)
Pseudo-second-order kinetic equation		
k_2 [g mg^{-1} h^{-1}]	2.1788	1.2539
q_e [mg g^{-1}]	0.5184	0.4939
$q_{e\ experimental}$	0.50	0.46
h_0 [mg g^{-1} h^{-1}]	0.5855	0.3059
r^2	0.9992	0.9995
Intraparticle diffusion kinetic equation		
k_{id1} [mg g^{-1} h$^{-0.5}$]	0.3189	0.2109
r_1^2	0.9956	0.9981
k_{id2} [mg g^{-1} h$^{-0.5}$]	0.1036	0.1234
r_2^2	0.9997	1.0
External diffusion kinetic equation		
k_{ext}, h^{-1}	0.2871	0.1875
r^2	0.9694	0.9811

The kinetic parameters calculated from studied models are listed in Table II.

The values of the correlation coefficient for both kinetic models showed that adsorption of both As(III) and As(V) species follows the pseudo-second-order model. The r^2 values close to 1.0 suggest that the process was controlled by chemisorption involving covalent or ionic bond formation. The similar sorption capacity in the acidic environment of both species was presumably due to occupation of the same active sites on the sorbent surface under acidic conditions, which confirms our previous considerations on the adsorption mechanism. Considering the rate constant of the pseudo-second-order model, it can be seen that the rate of As(III) adsorption is higher than As(V) removal, although arsenite adsorption is a more complex process. This fact may be caused by the presence of retained sulfonic groups contained in the hybrid polymer, which resulted in a Donnan exclusion effect toward As(V) anions. The negatively charged $-SO_3^-$ groups, covalently bound to the supporting polymer chains, inhibit permeation of arsenate anions into the hybrid polymer phase, where the majority of the precipitated manganese(IV) oxide is localized. This effect (the so-called Donnan membrane effect) results from the inability of the dissociated functional groups to diffuse out from the heterogeneous system.[58] This phenomenon may be the reason for slowing down of the arsenate adsorption process.

For identification of the rate limiting adsorption steps which are related to mass transport of adsorbate through the liquid film and sorbent porous structure, the kinetic data were further analyzed using adsorption diffusion models. The intraparticle diffusion model equation is expressed as follows:[54,59]

$$q_t = k_{id} t^{0.5} + c \quad (9)$$

If the plot of q_t versus $t^{0.5}$ is the straight line and the intercept c passes through the origin, the pore diffusion is the sole rate limiting step during the adsorption process, where k_{id} is the intraparticle diffusion rate constant (mg(g min)$^{-1}$). In practice, the intercept is rarely equal to zero, which indicates that the kinetic is also controlled by film diffusion; thus the value of c is proportional to the thickness of the boundary layer. As can be seen from Figure 9, the intraparticle diffusion model plots of As(III) and As(V) were multilinear, each portion of data points giving the straight line representing different steps of the adsorption process.

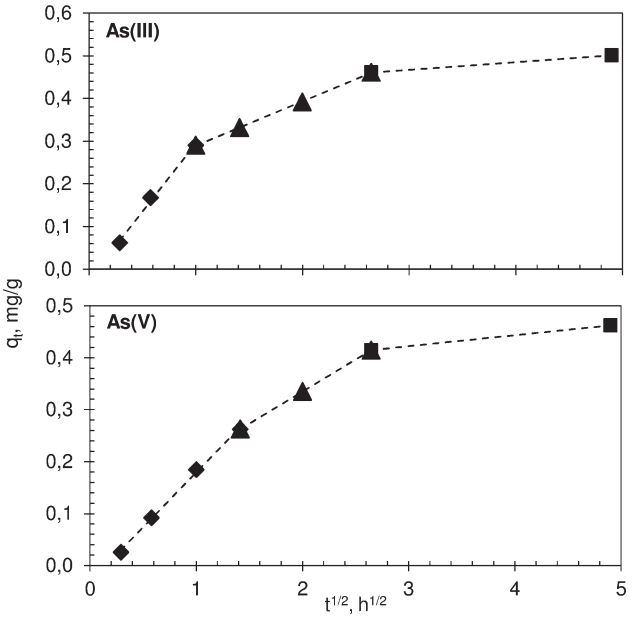

Figure 9. The plots of Intraparticle Diffusion Model for the adsorption of As(III) and As(V) on the R/S/Mn (10 mg As(III) dm^{-3}, 1.0 g of the R/S/Mn).

The adsorption of As(III) and As(V) followed three steps: the first line was presumably attributed to the boundary layer diffusion and the adsorption to the readily available sites on the external surface of the beads; the second portion represented the macropore and mesopore diffusion step which appears to be entirely controlled by the intraparticle diffusion mechanism; the third line was attributed to achieving the final equilibrium stage. The calculated kinetic parameters from the slopes are given in Table II. A noteworthy observation is the lower k_{id} value of As(V) adsorption at the initial stage which occurred within 2 h, in comparison to As(III) removal at the initial stage, which took place in the 1st h. This may be explained by the Donnan exclusion effect suggested before.

As the multistep nature of the adsorption process was observed for analysis of the initial stage kinetic data, we also used the external diffusion model, whose equation is given by:[57]

$$\ln[c_t/c_0] = k_{ext} t \quad (10)$$

where c_t is the concentration at time (t), c_0 is the initial concentration, and k_{ext} is the liquid film diffusion constant. The obtained linear plots in As(III) and As(V) adsorption at the initial time periods with correlation coefficients close to 1.0, and intercepts approximating zero, confirmed that film diffusion was the rate determining step.

Table III. Langmuir and Freundlich Isotherm Parameters for As(III) and As(V) Adsorption by R/S/Mn at Neutral pH

	Langmuir model		
	q_m [mg As g^{-1}]	K_L [dm^3 mg^{-1}]	r^2
As(III)	1.59	0.038	0.9979
As(V)	0.87	0.042	0.9944
	Freundlich model		
	K_F [dm^3 mg^{-1}]	$1/n$	r^2
As(III)	0.0595	0.8184	0.9985
As(V)	0.029	0.8446	0.9473

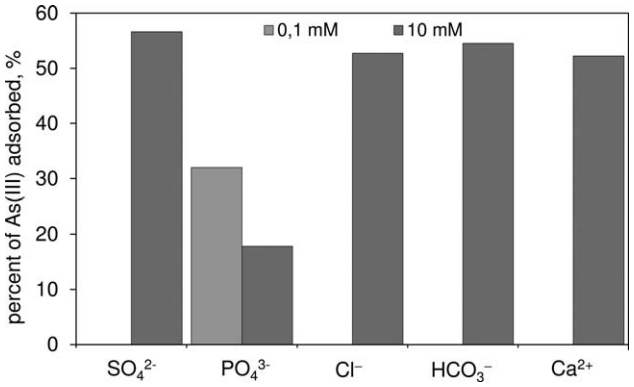

Figure 10. Effect of coexisting ions on As(III) removal by R/S/Mn; 40 cm^3 of $NaAsO_2$ solutions (5 mg As(III) dm^{-3}, 0.1 g of the R/S/Mn).

The data obtained from As(III) and As(V) adsorption isotherm experiments were described using Langmuir and Freundlich isotherm models, whose integrated equations are expressed, respectively:[33,60]

$$1/Q_e = 1/(Q_m \times K_L) \times 1/c_e + 1/Q_m \quad (11)$$

$$\log Q_e = \log K_F + 1/n \times \log c_e \quad (12)$$

where C_e is equilibrium adsorbate concentration in mg dm^{-3}, Q_e is equilibrium adsorption capacity in mg g^{-1}, K_F expressed in $mg^{1-(1/n)}(dm^3)^{1/n}$ g^{-1} and $1/n$ are Freundlich experimental constants, and Q_m and K_L are Langmuir experimental constants where Q_m is the maximum sorption capacity given in units of mg g^{-1} and K_L is the affinity of binding sites given in dm^3 mg^{-1}. The results of linear regression analyses shown in Table III indicate that adsorption of As(III) was better described by the Freundlich model.

This was not the case for As(V) adsorption data, which were best fitted with the Langmuir model. This observation is a consequence of a different mechanism of removal of these two species. Arsenate adsorption occurred due to the ion exchange reaction on the protonated sites, whose number was limited under constant pH conditions. The adsorption capacity of As(III) increased with its concentration, which was the result of sorbent surface modification due to the oxidation reaction, the mechanism of which was described earlier.

Effect of Coexisting Ions on Arsenite Oxidation and Adsorption

The presence of common ions coexisting with arsenic species may interfere with the oxidation and adsorption of As(III) and As(V), since certain ions may compete for manganese oxide active sites. Therefore, we also investigated the influence on these processes of cations and anions commonly existing in natural waters such as Ca^{2+}, Na^+, Cl^-, SO_4^{2-}, HCO_3^-, and PO_4^{3-}. As shown in Figure 10, only phosphates exhibit a distinct negative influence on arsenites sorption effectiveness.

Depending on PO_4^{3-} concentration in treated solution, the efficiency of the process dropped by 40–70%. The chemical properties of phosphates are similar to those of arsenates(V), resulting in competition for active sites on the MnO_2 surface. Because of close affinity of both species to mineral surfaces (iron, aluminum, and manganese oxides), the adverse impact of phosphates on arsenates sorption usually occurs in natural systems.[43,61] Despite the more complex, multistep mechanism of As(III) sorption on manganese oxide, ultimately arsenic is retained only as As(V);[42] therefore, the competition for active sites is between arsenates and phosphates.

As the oxidation of As(III) involves the initial adsorption of arsenite molecule on the MnO_2 surface, the presence of some competing ions, like phosphates, may decrease the efficiency of the oxidation reaction. However, the obtained results (not presented at the figure) showed, that the presence of Ca^{2+}, Na^+, Cl^-, SO_4^{2-}, HCO_3^-, and PO_4^{3-} ions, even at significantly higher concentration (10 m*M*) than arsenite (0.067 m*M*), had no influence on the As(III) oxidation capacity. In every case, the efficiency of the reaction reached almost 100%. The results obtained by Chiu and Hering[62] indicated that the competing effect of phosphates influenced the kinetics of the oxidation reaction rather than its final effectiveness. This can be explained by the reduced amount of active sites on the heterogeneous oxidant surface, which was the result of its passivation by adsorbed phosphates, in consequence slowing down the reaction rate.

Column Studies on As(III) Oxidation

The aim of the column studies was verification of the capacity of synthesized hybrid polymer for As(III) oxidation under conditions similar to those in natural waters. For that purpose, arsenite solution (1.0 mg As(III) dm^{-3}) containing some ions occurring in natural waters (Cl^-, SO_4^{2-}, PO_4^{3-}, HCO_3^-, Ca^{2+}, Mg^{2+}, Na^+) was passed through the polymer bed (m = 5 g, d = 10 mm, h = 120 mm) with the flow rate of 6 BV h^{-1}. To date, after 10 weeks of continuous work and after passing 94 dm^3 of the solution (9980 BV), the As(III) concentration in the effluent has not exceeded the level of 0.01 mg dm^{-3}. The working oxidation capacity obtained at this moment equals 18.8 mg As(III) g^{-1}.

The pH of the initial solution was about 7.5, whereas the pH in the first fractions of effluent decreased to 2.7–3.1, followed by settling at the level of 6.9–7.3. The initial drop of the pH of the effluent was a consequence of the hybrid polymer properties,

consisting of the capacity for acidification of the treated solution, which was explained earlier (3.2).

CONCLUSIONS

In this study, we examined the oxidative and sorptive properties of an MnO_2 loaded hybrid polymer ([P]-SO_2NH_2#MnO_2) toward arsenic species contained in water. The hybrid polymer was obtained using S/DVB copolymer having oxidizing functional groups as supporting material for manganese oxide deposition. In the single-step process, we obtained a product containing 7.3% Mn. The inorganic deposit of MnO_2 was evenly incorporated within the polymer matrix in the form of a thin film covering its surface. The batch studies showed that the hybrid polymer exhibited very high oxidizing capacity, even 75 mg g^{-1}, toward arsenite in the wide pH range of 2.0–12.0 and relatively low sorption capacity toward As(III) and As(V). This drawback can be overcome during the synthesis of hybrid polymer by coprecipitation with manganese oxide another inorganic deposit such as iron oxide exhibiting higher sorption capacity especially toward As(V) species. However, the low sorption capacity decreases the undesirable effect of passivation of the oxidant surface. This may result in a significantly prolonged period of operating time of the oxidizing fixed-bed system, which was confirmed in the column studies. The application of this material for arsenite oxidation under near-natural conditions representative of groundwater allowed for its total oxidation resulting in decrease of As(III) concentration from 1.0 mg dm^{-3} to below the detection limit—0.0015 mg dm^{-3}. The process is still running and after 2 months of continuous work resulted in 94 dm^3 (9980 BV) of purified solution. Thus, the obtained hybrid polymer may find application in arsenic adsorption processes as the pretreatment fixed oxidizing bed. Considering the practical uses of this material, the possibility of its regeneration becomes an important matter. As both passivation and reduction of the oxidant's surface take place during As(III) oxidation with manganese oxides, the regeneration process should include desorption of arsenate ions by alkalization of the active surface and reoxidation of Mn(II) to Mn(IV) with the use of a suitable oxidant. Research concerning this matter is currently underway.

ACKNOWLEDGMENTS

This research project was supported by the Ministry of Science and Higher Education of Poland in the years 2009-2012 (project No. N N523 418537).

REFERENCES

1. Celik, I.; Gallicchio, L.; Boyd, K.; Lam, T. K.; Matanoski, G.; Tao, X.; Shiels, M.; Hammond, E.; Chen, L.; Robinson, K. A.; Caulfield, L. E.; Herman, J. G.; Guallar, E.; Alberg, A. J. *Environ. Res.* **2008**, *108*, 48.
2. Clara, M.; Magalhaes, F. *Pure Appl. Chem.* **2002**, *74*, 1843.
3. Mandal, B. K.; Suzuki, K. T. *Talanta* **2002**, *58*, 201.
4. VillaescusaI, I.; Bollinger, J. C. *Rev. Environ. Sci. Biotechnol.* **2008**, *7*, 307.
5. Lee, G.; Song, K.; Bae, J. *Geochim. Cosmochim. Acta* **2011**, *75*, 4713.
6. Lescano, M. R.; Zalazar, C. S.; Cassano, A. E.; Brandi, R. J. *Photochem. Photobiol. Sci.* **2011**, *10*, 1797.
7. Neppolian, B.; Celik, E.; Choi H. *Environ. Sci. Technol.* **2008**, *42*, 6179.
8. Sorlini, S.; Gialdini, F. *Water Res.* **2010**, *44*, 5653.
9. Ghurye, G.; Clifford, D. J. *AWWA* **2004**, *96*, 84.
10. Bissen, M.; Frimmel, F. H. *Acta Hydrochim. Hydrobiol.* **2003**, *31*, 97.
11. Kim, M.-J.; Nriagu, J. *Sci. Total Environ.* **2000**, *247*, 71.
12. Mohan, D.; Pittman, C. U. J. *Hazard. Mater.* **2007**, *142*, 1.
13. Yang, H.; Lin, W.-Y.; Rajeshwar K. J. *Photochem. Photobiol. A* **1999**, *123*, 137.
14. Lee, H.; Choi, W. *Environ. Sci. Technol.* **2002**, *36*, 3872.
15. Emett, M. T, Khoe, G. H. *Water Res.* **2001**, *35*, 649.
16. Zaw, M.; Emett, M. T. *Toxicol. Lett.* **2002**, *133*, 113.
17. Rivera, J. F.; Bucher, Ch.; Saint-Aman, E.; Rivas, B. L.; Carmen Aguirre, M.; Sanchez, J.; Pignot-Paintrand, I.; Moutet, J.-C. *Appl. Catal. B-Environ.* **2013**, *129*, 130.
18. Rivas, B. L.; Carmen-Aquirre, M.; Pereira, E.; Bucher, Ch.; Royal, G.; Limosin, D.; Aman, E.; Moutet, J.-C. *Water Res.* **2009**, *43*, 515.
19. Zhao, X.; Zhang, B.; Liu, H.; Qu, J. J. *Hazard. Mater.* **2010**, *184*, 472.
20. Saleh, T. A.; Agarwal, S.; Gupta, V. K. *Appl. Catal. B-Environ.* **2011**, *106*, 46.
21. Zhang, G.; Liu, H.; Qu, J.; Jefferson, W. J. *Colloid Interf. Sci.* **2012**, *366*, 141.
22. Zhang, G.; Qu, J.; Liu, H.; Liu, R.; Li, G. *Environ. Sci. Technol.* **2007**, *41*, 4613.
23. Bajpai, S.; Chaudhuri, M. J. *Environ. Eng.* **1999**, *125*, 782.
24. Galaev, I. Y.; Mattiasson, B. *Trends Biotechnol.* **1999**, *17*, 335.
25. Gangopadhyay, R.; De, A. *Chem. Mater.* **2000**, *12*, 608.
26. Hristovski, K.; Westerhoff, P.; Moller, T.; Sylvester, P.; Condit, W.; Mash, H. J. *Hazard. Mater.* **2008**, *152*, 397.
27. Iesan, C. M.; Capat, C.; Ruta, F.; Udrea, I. *React. Funct. Polym.* **2008**, *68*, 1578.
28. Pan, B.; Pan, B.; Zhang, W.; Lv, L.; Zhang, Q.; Zheng, S. *Chem. Eng. J.* **2009**, *151*, 19.
29. Burnett, J. L.; Croudace, I. W.; Warwick, P. E. *Environ. Earth Sci.* **2012**, *67*, 637.
30. Lenoble, V.; LacLautre, Ch.; Serpaud, B.; Deluchat, V.; Bollinger, J. C. *Sci. Total Environ.* **2004**, *326*, 197.
31. Lenoble, V.; Chabroullet, Ch.; Shukry, R.; Serpaud, B.; Deluchat, V.; Bollinger, J.-C. *J. Colloid Interf. Sci.* **2004**, *280*, 62.
32. Varga, Z. *Appl. Radiat. Isotopes* **2007**, *65*, 1095.
33. Wan, S.; Zhao, X.; Lv, L.; Su, Q.; Gu, H.; Pan, B.; Zhang, W.; Lin, Z.; Luan, J. *Ind. Eng. Chem. Res.* **2010**, *49*, 7574.
34. Ciechanowska, A. A Studies on Reactions of N-Halogenosulfonamide Derivatives of Poly(styrene-divinylbenzene)

Copolymers with Fe(II) and Mn(II) Cations. Ph.D. Thesis, Wroclaw University of Economics, Wrocław, December **2008**.

35. Kociołek-Balawejder, E.; Ciechanowska, A.; Ociński, D.; Stanisławska, E. *Pat. Pol. 388*, 431, July 01, **2009**.
36. Bogoczek, R.; Kociołek-Balawejder, E. *Angew. Makromol. Chem.* **1991**, *188*, 85.
37. Newcombe, G.; Hayes, R.; Drikas, M. *Colloids Surf. A* **1993**, *78*, 65.
38. Lenoble, V.; Deluchat, V.; Serpaud, B.; Bollinger, J.-C. *Talanta* **2003**, *61*, 267.
39. Johnson, D. L.; Pilson, M. E. Q. *Anal. Chim. Acta* **1972**, *58*, 289.
40. Kim, M.-J. *Bull. Environ. Contam. Toxicol.* **2001**, *67*, 46.
41. Ciechanowska, A.; Hanuza, J.; Kociołek-Balawejder, E.; Stanisławska, E. *Mater. Chem. Phys.* **2012**, *132*, 870.
42. Manning, B. A.; Fendorf, S. E.; Bostick, B.; Suarez, D. L. *Environ. Sci. Technol.* **2002**, *36*, 976.
43. Zhu, M.; Paul, K. W.; Kubicki, J. D.; Sparks, D. L. *Environ. Sci. Technol.* **2009**, *43*, 6655.
44. Lafferty, B. J.; Ginder-Vogel, M.; Sparks, D. L. *Environ. Sci. Technol.* **2010**, *44*, 8460.
45. Tournassat, Ch.; Charlet, L.; Bosbach, D.; Manceau, A. *Environ. Sci. Technol.* **2002**, *36*, 493.
46. Moore, J. N.; Walker, J. R.; Hayes, T. H. *Clays Clay Miner.* **1990**, *38*, 549.
47. Nesbitt, H. W.; Canning, G. W.; Bancroft, G. M. *Geochim. Cosmochim. Acta* **1998**, *62*, 2097.
48. Power, L. E.; Arai, Y.; Sparks, D. L. *Environ. Sci. Technol.* **2005**, *39*, 181.
49. Li, X.-j.; Liu, Ch.-s.; Li, F.-b.; Li, Y.-t.; Zhang, L.-j.; Liu, Ch.-p.; Zhou, Y.-z. *J. Hazard. Mater.* **2010**, *173*, 675.
50. Scott, M. J.; Morgan, J. J. *Environ. Sci. Technol.* **1995**, *29*, 1898.
51. Lafferty, B. J.; Ginder-Vogel, M.; Sparks, D. L. *Environ. Sci. Technol.* **2011**, *45*, 9218.
52. Lafferty, B. J.; Ginder-Vogel, M.; Zhu, M.; Livi, K. J. T.; Sparks, D. L. *Environ. Sci. Technol.* **2010**, *44*, 8467.
53. Driehaus, W.; Seith, R.; Jekel, M. *Water Res.* **1995**, *29*, 297.
54. Qiu, H.; Lv, L.; Pan, B.-c.; Zhang, Q.-j.; Zhang, W.-m.; Zhang, Q.-x. *J. Zhejiang University Sci. A* **2009**, *10*, 716.
55. Bhakat, P. B.; Gupta, A. K.; Ayoob, S.; Kundu, S. *Colloid Surf.* **2006**, *281*, 237.
56. Ho, Y.-S. *J. Hazard. Mater.* **2006**, *B136*, 681.
57. Castro Lopez, M.; Cela Perez, M. C.; Dopico Garcia, M. S.; Lopez Vilarino, J. M.; Gonzales Rodriguez, M. V.; Barral Losada, L. F. *Anal. Chim. Acta* **2012**, *721*, 68.
58. Cumbal, L.; Sengupta, A. K. *Environ. Sci. Technol.* **2005**, *39*, 6508.
59. Cheung, M. H.; Szeto, Y. S.; McKay, G. *Bioresource Technol.* **2007**, *98*, 2897.
60. Ntim, S. A.; Mitra, S. J. *Chem. Eng. Data* **2011**, *56*, 2077.
61. Ma, H.; Zhu, Z.; Dong, L.; Qiu, Y.; Zhao, J. *Sep. Sci. Technol.* **2011**, *46*, 130.
62. Chiu, V. Q.; Hering, J. G. *Environ. Sci. Technol.* **2000**, *34*, 2029.